Guanidination of notexin alters its membrane-damaging activity in response to sphingomyelin and cholesterol

Pei-Hsiu Kao[1], Yi-Ling Chiou[1], Shinne-Ren Lin[2] and Long-Sen Chang[1,*]

[1]*Institute of Biomedical Sciences, National Sun Yat-Sen University-Kaohsiung Medical University Joint Research Center, National Sun Yat-Sen University, Kaohsiung 804, Taiwan*

[2]*Department of Medicinal and Applied Chemistry, Kaohsiung Medical University, Kaohsiung 807, Taiwan*

**Corresponding author (Fax, 886-7-5250197; Email, lschang@mail.nsysu.edu.tw)*

To elucidate the contribution of phospholipase A_2 (PLA_2) activity of notexin to its ability to perturb membranes, comparative studies on the interaction of notexin and guanidinated notexin (Gu-notexin) with egg yolk phosphatidylcholine (EYPC), EYPC/egg yolk sphingomyelin (EYSM) and EYPC/EYSM/cholesterol vesicles were conducted. EYSM notably reduced the membrane-damaging activity of notexin against EYPC vesicles, but had an insignificant influence on that of Gu-notexin. Unlike the effects noted with notexin, inactivation of PLA_2 activity by EDTA led to a reduction in the ability of Gu-notexin to induce EYPC/EYSM vesicle leakage and to increase Gu-notexin-induced membrane permeability of EYPC/EYSM/cholesterol vesicles. The geometrical arrangement of notexin and Gu-notexin in contact with either EYPC/EYSM vesicles or EYPC/EYSM/cholesterol vesicles differed. Moreover, global conformation of notexin and Gu-notexin differed in either Ca^{2+}-bound or metal-free states. These results indicate that notexin and Gu-notexin could induce membrane permeability without the involvement of PLA_2 activity, and suggest that guanidination alters the membrane-bound mode of notexin on damaging phospholipid vesicles containing sphingomyelin and cholesterol.

[Kao P-H, Chiou Y-L, Lin S-R and Chang L-S 2010 Guanidination of notexin alters its membrane-damaging activity in response to sphingomyelin and cholesterol; *J. Biosci.* **35** 583–593] **DOI** 10.1007/s12038-010-0067-6

1. Introduction

Notexin, a presynaptic phospholipase A_2 (PLA_2) neurotoxin purified from the venom of *Notechis scutatus scutatus*, is a basic protein with 119 amino acids and 7 disulphide bridges (Westerlund *et al*. 1992). Apart from its presynaptic neurotoxicity, which blocks neuromuscular transmission by affecting the release of acetylcholine, notexin exhibits PLA_2 activity and myotoxicity (Rigoni *et al.* 2004; Plant *et al.* 2006). X-ray crystallographic analyses reveal that notexin is structurally homologous to PLA_2 enzymes from the mammalian pancreas and snake venom (Westerlund *et al*. 1992).

As presynaptic PLA_2 neurotoxins show both PLA_2 activity and presynaptic neurotoxicity (Harris 1991), it is important to clarify the role of enzymatic activity in inducing the toxic effect. There is considerable evidence in favour of the essential role of PLA_2 activity involved in presynaptic neurotoxicity (Harris 1991; Rigoni *et al.* 2005). Nevertheless, there is no quantitative relationship between PLA_2 activity and presynaptic potency (Wilson and Nicholson 1997; Rosenberg 1997; Rigoni *et al.* 2004; Paoli *et al.* 2009). Chemical modification studies with presynaptic PLA_2 neurotoxins show a dissociation of enzymatic activity from lethal toxicity (Yang 1997). Taken together, it is likely that a catalytic activity-independent mechanism contributes

Keywords. Cholesterol; guanidination; membrane-damaging activity; notexin; phospholipase A_2; sphingomyelin.

Abbreviations used: CD, circular dichroism; EYPC, egg yolk phosphatidylcholine; EYSM, egg yolk sphingomyelin; FTIR, Fourier transform infrared; PLA_2, phospholipase A_2

at least in part to the cytotoxicity and pharmacological activities of presynaptic neurotoxins.

The outer-membrane leaflet of mammalian cells is composed mainly of phosphatidylcholine, sphingomyelin and cholesterol (Gurr *et al.* 2002). Previous studies indicated that the presence of sphingomyelin inhibits the enzymatic activity of human-secreted PLA_2 against phosphatidylcholine (Koumanov *et al.* 1998; Gesquiere *et al.* 2002). Moreover, packing sphingomyelin and cholesterol relieves the inhibitory effect of sphingomyelin on PLA_2 activity (Koumanov *et al.* 1998). Noticeably, Paoli *et al.* (2009) found that the PLA_2 activity of presynaptic neurotoxins on cultured neurons was at least 100-fold lower than their activity on synthetic substrate, the 1,2-dithio analogue of di-heptanoyl phosphatidylcholine. Moreover, their studies suggest that the main site of action of notexin and other presynaptic PLA_2 neurotoxins is the outer layer of the plasma membrane. Thus, studies on the interaction of notexin with phosphatidylcholine/sphingomyelin and phosphatidylcholine/sphingomyelin/cholesterol vesicles may provide clues to elucidate the contribution of PLA_2 activity to damage membrane. Guanidination of notexin caused a reduction in its PLA_2 activity (Yang and Chang 1990). Investigation into the ability of guanidinated notexin (Gu-notexin) to induce membrane permeability should throw more light on the PLA_2 activity association with membrane-damaging activity. Our data revealed that the ability of notexin and Gu-notexin to damage phospholipid vesicles was affected in different ways by sphingomyelin and cholesterol. This suggested that PLA_2 activity, membrane-bound mode and phospholipid compositions contributed unequally to the membrane-damaging activity of notexin and Gu-notexin.

2. Materials and methods

Notexin was purified from *Notechis scutatus scutatus* venom according to the procedure described previously (Chang 1996). Guanidination of notexin with *O*-methylisourea was prepared according to the procedure described in Yang and Chang (1990). Calcein, cholesterol, EDTA, egg yolk phosphatidylcholine (EYPC) and egg yolk sphingomyelin (EYSM) were purchased from Sigma-Aldrich Inc., and 10, 12-tricosadiynoic acid was obtained from Fluka. 1,2-bis-(1-pyrene- decanoyl)-sn-glycero-3-phosphocholine (bisPy-PC) and N-(fluorescein-5- thiocarbamoyl)-1,2-dihexadecanoyl-phosphatidylethanolamine (FPE) were the products of Molecular Probes, and 1-palmitoyl-2-(6,7-dibromostearoyl) phosphatidylcholine (6,7-Br_2PC), 1-palmitoyl-2-(9,10-dibromostearoyl) phosphatidylcholine (9,10-Br_2PC) and 1-palmitoyl-2-(11,12-dibromostearoyl) phosphatidylcholine (11,12-Br_2PC) were from Avanti Polar Lipids. Sepharose 6B was obtained from Amersham Biosciences. All other reagents were products of analytical grade.

2.1 *PLA_2 activity assay*

PLA_2 activity was measured by a fluorescence assay, using vesicles that contained 5 mol% bisPy-PC. The vesicles were prepared by extrusion through 100 nm polycarbonate membrane. A fluorescence spectrum of vesicles with bisPy-PC was measured between 360 and 500 nm using an excitation wavelength at 347 nm. All measurements were conducted under constant stirring. The emission spectrum of monomeric pyrene had two peaks around 378 and 396 nm, whereas the proximity of pyrene moieties resulted in a strong excimer peak around 470 nm (Ray *et al.* 2007). Lipid hydrolysis by notexin caused a decrease in the excimer signal at 470 nm and increase in the monomer signal at 378 nm and 396 nm because of the two pyrene moieties separated from each other. The activity was calculated as $R_t/R_0 - 1$, where R_t is the ratio of fluorescence intensities at 378 and 470 nm at time t, $R_t = (F_{378}/F_{470})_t$, and R_0 is R_t before addition of notexin.

2.2 *Release of entrapped fluorescent markers from liposomes*

Membrane-damaging activity was determined by measuring the release of the liposome-entrapped, self-quenching fluorescent dye calcein according to the procedure described by Kao *et al.* (2007). Loss of liposome membrane integrity results in dilution of the fluorophore, with a consequent increase in the fluorescence signal. Lipid mixtures with indicated compositions were dissolved in chloroform/methanol (v/v, 2:1) at a molar ratio of 9:1 and dried by evaporation. Buffer (10 mM Tris-HCl, 100 mM NaCl, pH 7.5, with 5 mM $CaCl_2$ or 5 mM EDTA) containing 50 mM calcein was added to the film of lipids, and after hydration the suspension was shaken vigorously. The multilamellar vesicles obtained in this way were extruded 10 times, above the transition temperature, through a 100 nm polycarbonate filter and applied to a Sepharose 6B column (2 × 15 cm) to separate the liposome from the free calcein. Leakage was induced by adding aliquots of toxin to a vesicle suspension directly in the cuvette used for fluorescence determination at 30°C. The kinetics of membrane damage was monitored by the increase in fluorescence with emission at 520 nm and excitation at 490 nm, and the signal was expressed as percentage of total calcein release after the addition of 0.2% Triton X-100.

2.3 *Lipid-binding experiments*

FPE was incorporated at 2 mol% into EYPC/EYSM or EYPC/EYSM/cholesterol vesicles, which were prepared by extrusion through 100 nm pore size polycarbonate filters.

Excitation was at 490 nm, and emission intensity at 515 nm was monitored. Binding of notexin with phospholipid vesicles (8.14 μM) caused an increase in fluorescence emission intensity (ΔF) of FPE.

2.4 *Colorimetric phospholipid/polydiacetylene membrane assay*

The penetration of notexin into phospholipid/polydiacetylene (PDA) vesicles was detected according to the methods described by Kolusheva *et al.* (2008). EYPC/EYSM/10,12-tricosadiynoic acid (4.9:2.1:3 molar ratio) or EYPC/EYSM/cholesterol/10,12-tricosadiynoic acid (3.43:1.47:2.1:3 molar ratio) was dissolved in chloroform/ethanol (1:1, v/v) and dried together *in vacuo* followed by addition of de-ionized water and sonication at 70°C. The vesicle solution was then cooled to room temperature and kept at 4°C overnight. The vesicles were then polymerized using irradiation at 254 nm for 30–40 s, with the resulting phospholipid/PDA solution exhibiting an intense blue colour. Vesicle samples for experiments were prepared at a concentration of 0.5 mM (total lipid) in 10 mM Tris-HCl–100 mM NaCl (pH 7.5) containing 5 mM Ca^{2+} or 5 mM EDTA. Following the addition of notexin, the changes in absorbance at 500 nm and 640 nm of vesicle solution were measured.

A quantitative value for the extent of blue-to-red colour transitions within the vesicle solutions is given by the colorimetric response (%CR), which is defined as follows: $\%CR = [(PB_0 - PB_1)/PB_0] \times 100$, where $PB = A_{640}/(A_{640} + A_{500})$, A_{640} and A_{500} are the absorbance measured at 640 nm and 500 nm, respectively. PB_0 is the A_{640}/A_{500} ratio of the control sample (before the addition of notexin), and PB_1 is the value obtained for the vesicle solution after the addition of notexin. All reported %CR values were averages of six independent measurements.

2.5 *Circular dichroism measurement*

Circular dichroism (CD) spectra were obtained on a Jasco J-810 spectropolarimeter with a cell path-length of 0.5 mm. The CD spectra were measured from 260 nm to 190 nm, and CD spectra were obtained by averaging the signals of five scans.

2.6 *Analyses of Fourier transform infrared spectra of notexin and Gu-notexin*

Fourier transform infrared (FTIR) spectra were measured using a 66 v/s FTIR spectrometer (Bruker Optics). Notexin and Gu-notexin were dissolved in D_2O-based buffer containing 10 mM HEPES–100 mM NaCl (pH 7.5) with 5 mM $CaCl_2$ or 5 mM EDTA. Then, the samples were transferred to a demountable cell composed of two CaF_2 windows separated by a 25 μm Teflon spacer clamped together in a brass holder. The FTIR spectra were recorded at a spectral resolution of 2 cm^{-1} for 200 scans, and then inverted to second-derivative spectra.

2.7 *Fluorescence measurement*

The fluorescence intensity was measured by a Hitachi model 4500 spectrophotofluorometer using a 5 nm slit width. All measurements used a 1 cm path-length and were performed in a total volume of 2 ml of 10 mM Tris-HCl–100 mM NaCl (pH 7.5) containing 5 mM Ca^{2+} or 5 mM EDTA. An excitation wavelength at 295 nm was employed to selectively excite the Trp residues.

2.8 *Quenching of Trp residues by brominated phosphatidylcholines*

The depth of membrane insertion of notexin and Gu-notexin was determined by using differential quenching of Trp fluorescence by Br_2PCs brominated at the 6,7-, 9,10- or 11,12-positions of sn-2 acyl chain. Trp fluorescence spectra of toxins were measured in the presence of EYPC/EYSM and EYPC/EYSM/cholesterol vesicles with and without 20 mol% Br_2PCs in 10 mM Tris-HCl–100 mM NaCl (pH 7.5). In the distribution analysis, the depth of the Trp residues was calculated by fitting the data to the following equation (Zhao and Kinnunen 2002):

$$\ln F_o/F = [S/\sigma(2\pi)^{1/2}] \cdot \exp[-(h-h_m)^2/2\sigma^2].$$

Where F_o and F represent the fluorescence intensities without and with the quencher, S is the area under the distribution curve (a measurement of the effectiveness of quenching), σ is the dispersion (the half-width at half) of the distribution curve, h_m is the most probable location of the fluorophore (Trp residues) with respect to the membrane center and h is the average bromine distances from the bilayer center, taken to be 11.0, 8.3 and 6.5 Å for 6,7-, 9,10- and 11,12-Br_2PCs, respectively (Mclntosh and Holloway 1987; Ladokhin 1997).

3. Results and discussion

The fluorescence intensity of FPE is sensitive to the ionization state of the carboxyl group of fluorescein, and the emission intensity increases with increasing deprotonation (Wall *et al.* 1995). Absorption of cationic protein to the membrane reduces the negative surface charge of the membrane and causes deprotonation of the carboxyl group of fluorescein, leading to an increase in FPE fluorescence intensity (Qin *et al.* 2005). Once the protein comes into

contact with the membrane, changes in FPE fluorescence intensity also report the protein reorganization events that arise from a modification of the charged profiles present at the membrane–water interface (Wall *et al.* 1995). As shown in figure 1, the FPE fluorescence intensity increased with increasing notexin or Gu-notexin concentrations. The FPE fluorescence enhancement by notexin or Gu-notexin binding with FPE/EYPC/EYSM/cholesterol vesicles was different from that with FPE/EYPC/EYSM vesicles regardless of the presence of Ca^{2+}. This indicated that the geometrical arrangement of notexin and Gu-notexin in contact with EYPC/EYSM/cholesterol was different from that with EYPC/EYSM. Moreover, the fluorescence intensity enhancement of FPE/EYPC/EYSM or FPE/EYPC/EYSM/cholesterol vesicles by notexin and Gu-notexin was not the same, suggesting that conformation and/or orientation of Gu-notexin on the water–lipid interface were different from those of notexin.

Previous studies have indicated that lipid/PDA vesicles mimic the cellular membrane environment and provide information on the binding of pore-forming peptides with the membrane (Kolusheva *et al.* 2000a,b). The blue-to-

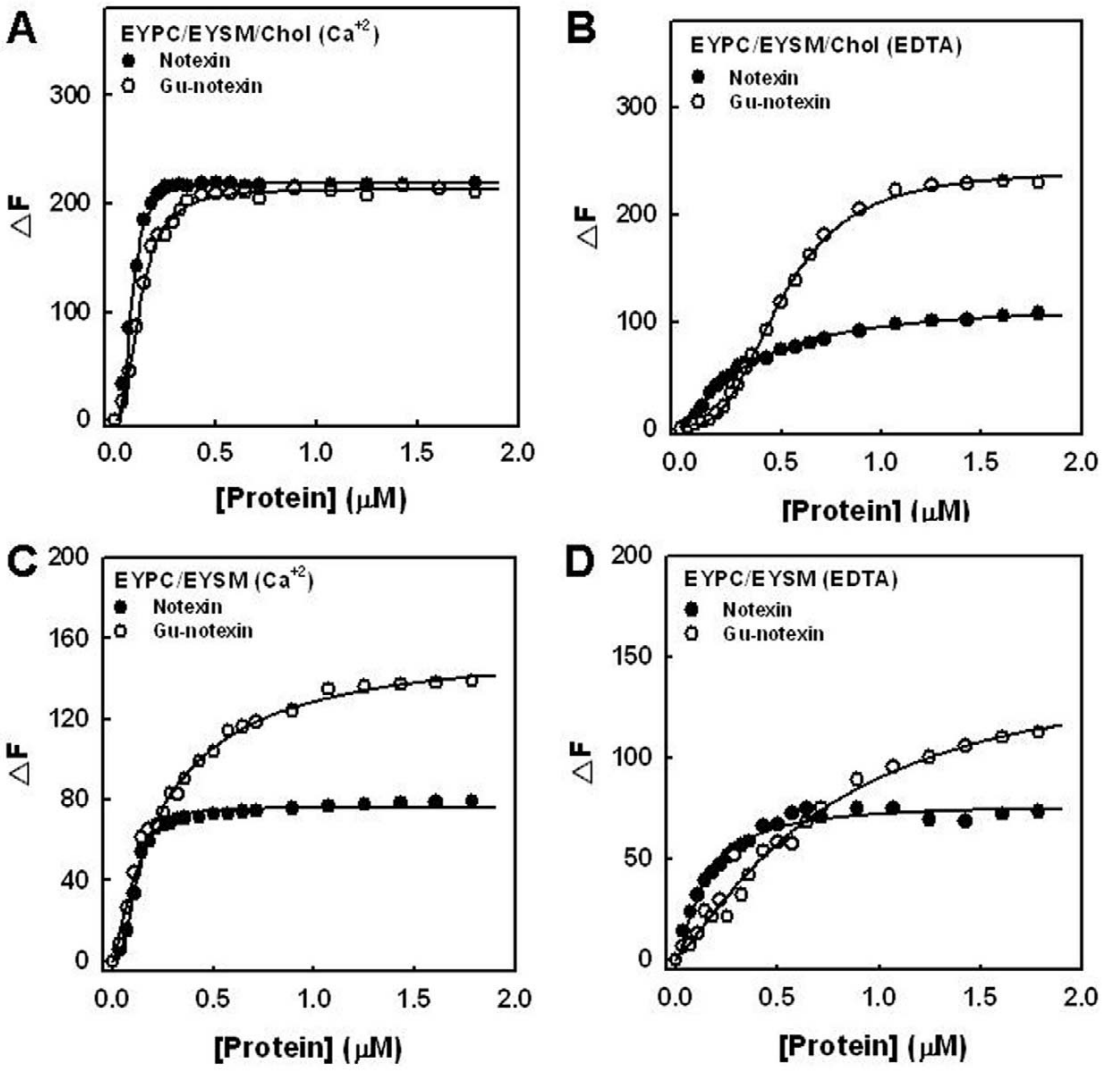

Figure 1. The binding of notexin and Gu-notexin with FPE/EYPC/EYSM and FPE/EYPC/EYSM/cholesterol vesicles enhanced the fluorescence intensity of FPE. The experiments were performed in 10 mM Tris-HCl–100 mM NaCl (pH 7.5) containing 5 mM Ca^{2+} (**A**, **C**) or 5 mM EDTA (**B**, **D**) . (**A**, **B**) EYPC/EYSM/cholesterol (mol/mol/mol, 49/21/30) and (**C**, **D**) EYPC/EYSM (mol/mol, 70/30) vesicles were used in the present experiments. The abbreviation Chol represents cholesterol. The symbols ● and ○ represent the binding of phospholipid vesicles with notexin and Gu-notexin, respectively.

red transformation in lipid/PDA vesicles depended on the disruption of the lipid interface by membrane-interacting compounds and on their penetration depth into the lipid bilayer (Kolusheva *et al.* 2000b). Peptides that preferably disrupted the lipid head-group region induced more pronounced color transitions (Kolusheva *et al.* 2000b, 2008). Thus, a higher colorimetric response (%CR) reflected a greater lipid–surface interaction. As shown in Figure 2, notexin or Gu-notexin binding with lipid/PDA vesicles resulted in increased %CR. Compared with notexin, Gu-notexin induced a notable increase in color transition of EYPC/EYSM/PDA or EYPC/EYSM/cholesterol/PDA vesicles either in the absence or presence of Ca^{2+}. The colorimetric response (%CR) of EYPC/EYSM/PDA vesicles upon binding with Ca^{2+}-bound or metal-free toxins was different from that of EYPC/EYSM/cholesterol/PDA vesicles, implying distinctive modes of interactions between notexin and Gu-notexin with the vesicle interface. To

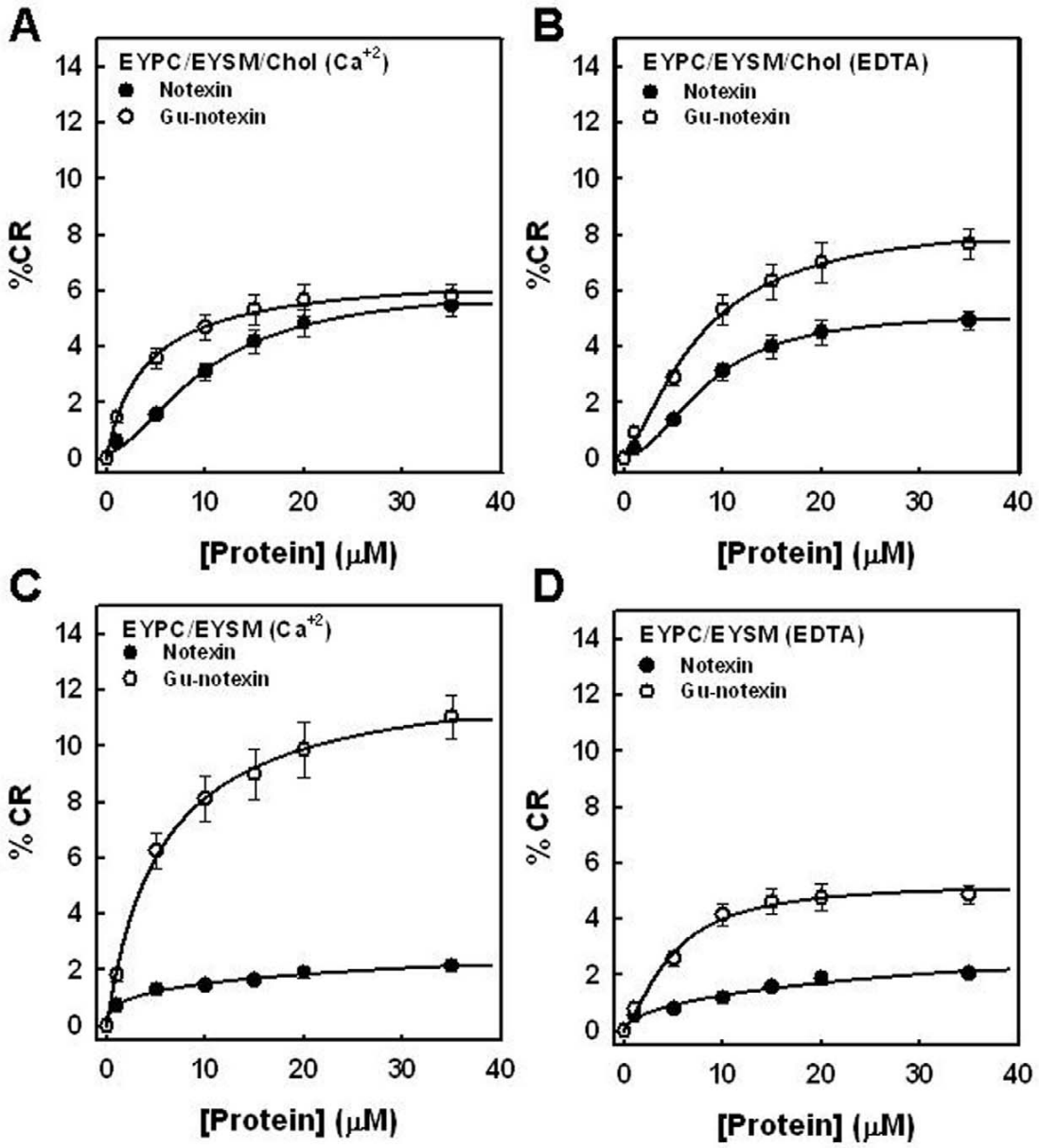

Figure 2. Colorimetric dose–response curve of EYPC/EYSM/PDA and EYPC/EYSM/cholesterol/PDA vesicles titrated with notexin and Gu-notexin. The experiments were conducted essentially according to the procedure described in Materials and Methods section. All reported %CR values were averages of six independent measurements.

further examine the membrane-bound mode of notexin and Gu-notexin, intrinsic fluorescence quenching of notexin and Gu-notexin by bromine-labelled lipids was conducted Figure 3 shows that the Trp fluorescence of EYPC/EYSM/cholesterol-bound or EYPC/EYSM-bound toxins was not equally quenched by bromine-labelled lipids. Upon binding with EYPC/EYSM/cholesterol vesicles, Trp fluorescence of notexin and Gu-notexin was more susceptible to quenching by 6,7-Br_2PC and 9,10-Br_2PC (figure 3A and 3B). Compared with that of Ca^{2+}-bound notexin, the intrinsic fluorescence of Ca^{2+}-bound Gu-notexin was notably quenched upon binding with EYPC/EYSM vesicles (figure 3C and 3D). The accessibility of Trp residues in Ca^{2+}-bound Gu-notexin for 9,10-Br_2PC and 11,12-Br_2PC was higher than that for 6,7-

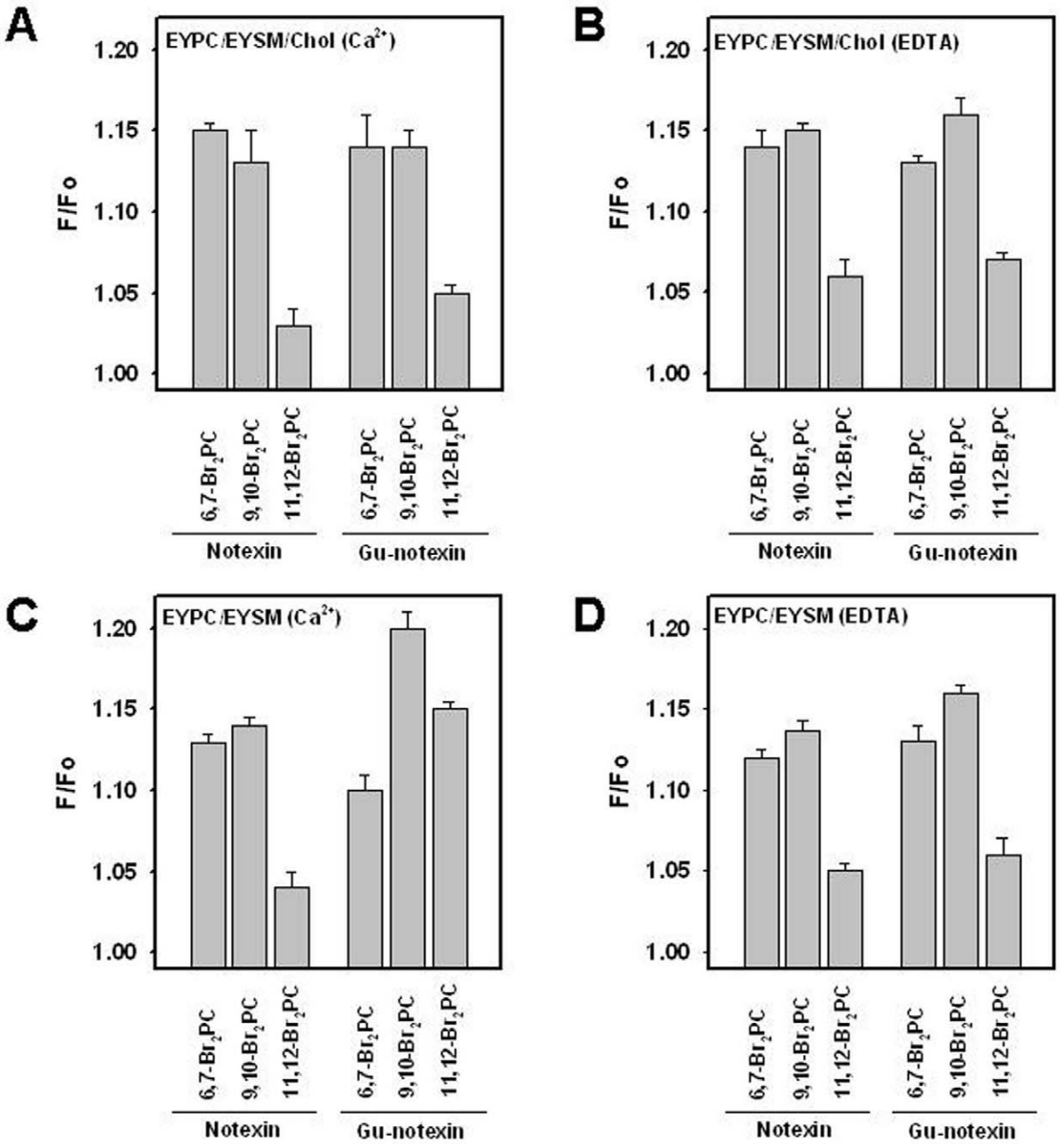

Figure 3. Quenching of Trp fluorescence of notexin and Gu-notexin by brominated lipids. The experiments were performed in 10 mM Tris-HCl–100 mM NaCl (pH 7.5) containing 5 mM Ca^{2+} or 5 mM EDTA. Trp fluorescence of notexin and Gu-notexin were measured in the presence of unlabelled phospholipid vesicles (F_o) and in the presence of phospholipd vesicles containing 20 mol% 6,7-, 9,10- or 11,12-Br_2PCs (F). The concentration of toxins and phospholipid vesicles were 7.1 μM and 213 μM, respectively. (**A**, **B**) Quenching of Trp fluorescence of Ca^{2+}-bound and metal-free toxins upon binding with EYPC/EYSM/cholesterol vesicles containing 6,7-, 9,10- or 11,12-Br_2PCs. (**C**, **D**) Quenching of Trp fluorescence of Ca^{2+}- bound and metal-free toxins upon binding with EYPC/EYSM vesicles containing 6,7-, 9,10- or 11,12-Br_2PCs.

Br_2PC in EYPC/EYSM vesicles, while that of metal-free Gu-notexin for 6,7-Br_2PC and 9,10-Br_2PC was higher than that for 11,12-Br_2PC (figure 3C and 3D). From these data, the penetration depth (h_m) of Trp residues was calculated. Trp residues of Ca^{2+}-bound notexin, Ca^{2+}-bound Gu-notexin, metal-free notexin and metal-free Gu-notexin resided in EYPC/EYSM/cholesterol vesicles at distances of 9.81±0.02 Å, 9.65±0.03 Å, 9.54±0.04 Å and 9.33±0.02 Å, respectively, from the center of the bilayer. Alternatively, the bilayer penetration depth of Trp residues into EYPC/EYSM vesicles was 9.56±0.06 Å, 9.16±0.04 Å, 9.45±0.05 Å and 9.37±0.05 Å for Ca^{2+}-bound notexin, Ca^{2+}-bound Gu-notexin, metal-free notexin and metal-free Gu-notexin, respectively. Given that notexin and Gu-notexin exhibited significant penetration depth differences upon binding with EYPC/EYSM/cholesterol vesicles and EYPC/EYSM vesicles, it again suggested distinctive modes of interactions between notexin and Gu-notexin with the vesicle interface. In view of that notexin contains two Trp residues at positions 20 and 110, the quenching of Trp fluorescence by brominated lipids could not conclusively delineate the depth of either Trp-20 or Trp-110 residing in EYPC/EYSM/cholesterol vesicles and EYPC/EYSM vesicles.

Conformation of Ca^{2+}-bound and metal-free toxins was further analysed using amide I band of the FTIR spectra. The amide I region (1600–1700 cm^{-1}) in the FTIR spectrum contains contributions from the C=O stretching vibration of the amide group (about 80%) with a minor contribution from the C–N stretching vibration (Susi *et al.* 1985; Surewicz *et al.* 1993). Thus, alteration in secondary structure leads to a change in the amide I band of the FTIR spectrum. As shown in figure 4, the FTIR spectra of notexin and Gu-notexin differed regardless of the presence of Ca^{2+}. Moreover, the binding of Ca^{2+} caused a change in conformation of notexin and Gu-notexin distinct from their metal-free state. Obviously, global conformation of Ca^{2+}-bound toxin and metal-free toxin differed. Figures 5A–B show that intrinsic fluorescence intensity and emission maximum wavelength differed between Ca^{2+}-bound toxins and metal-free toxins, suggesting that Ca^{2+}-binding induced changes in the gross conformation of notexin and Gu-notexin. This suggestion was also supported by the findings that the CD spectra of Ca^{2+}-bound toxins significantly differed from those of metal-free toxins (figure 5C and 5D).

Given that Ca^{2+} is a co-factor for catalytic activity of PLA_2 enzymes and presynaptic PLA_2 neurotoxins, the binding of Ca^{2+} with notexin or removal of Ca^{2+} by EDTA either triggers or halts PLA_2 activity, respectively. It was found that the percentage of calcein released from EYPC vesicles caused by Ca^{2+}-bound notexin and Gu-notexin were 19.0±1.3% and 13.8±0.3%, respectively (figure 6A). The membrane-damaging activity of metal-free notexin and Gu-notexin against EYPC vesicles were 4.7±0.2% and 1.5±0.2%, respectively. Increased EYSM content ranging from 10 mol% to 50 mol% in EYPC vesicles caused a marked reduction in calcein release induced by Ca^{2+}-bound notexin, while the ability of Ca^{2+}-bound or metal-free Gu-notexin to damage EYPC vesicles and EYPC/EYSM vesicles was similar. Metal-free notexin showed similar activity toward EYPC and EYPC/EYSM vesicles, while metal-free Gu-notexin-induced permeability in EYPC/EYSM vesicles were higher than that in EYPC vesicles (figure 6B). These results suggested that guanidination of notexin promoted a preference for damaging EYPC/EYSM vesicles. To examine

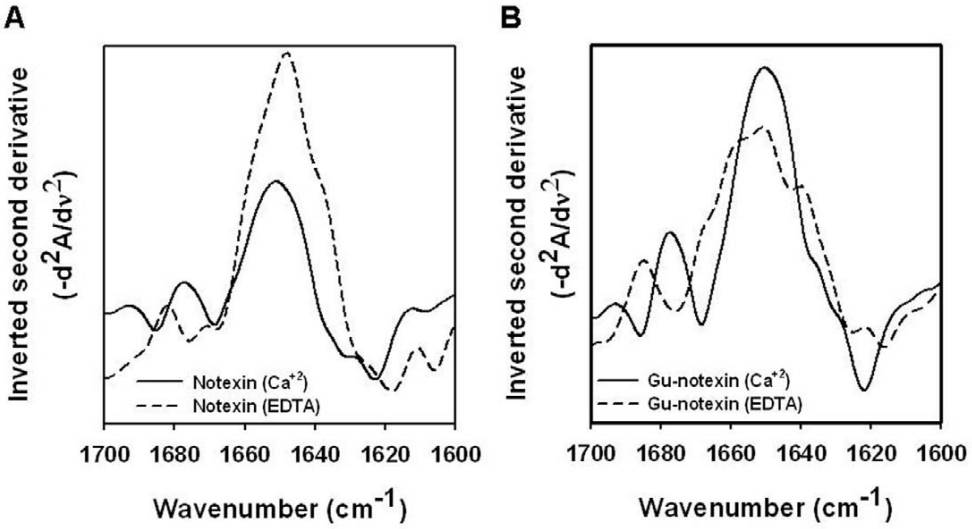

Figure 4. Inverted second-derivative amide I spectra of notexin and Gu-notexin. The second-derivative of FTIR spectra in the amide I region of notexin and Gu-notexin were measured in the presence of 5 mM Ca^{2+} (solid line) and 5 mM EDTA (short line). The buffer composition was 10 mM HEPES–100 mM NaCl in D_2O (pH 7.5).

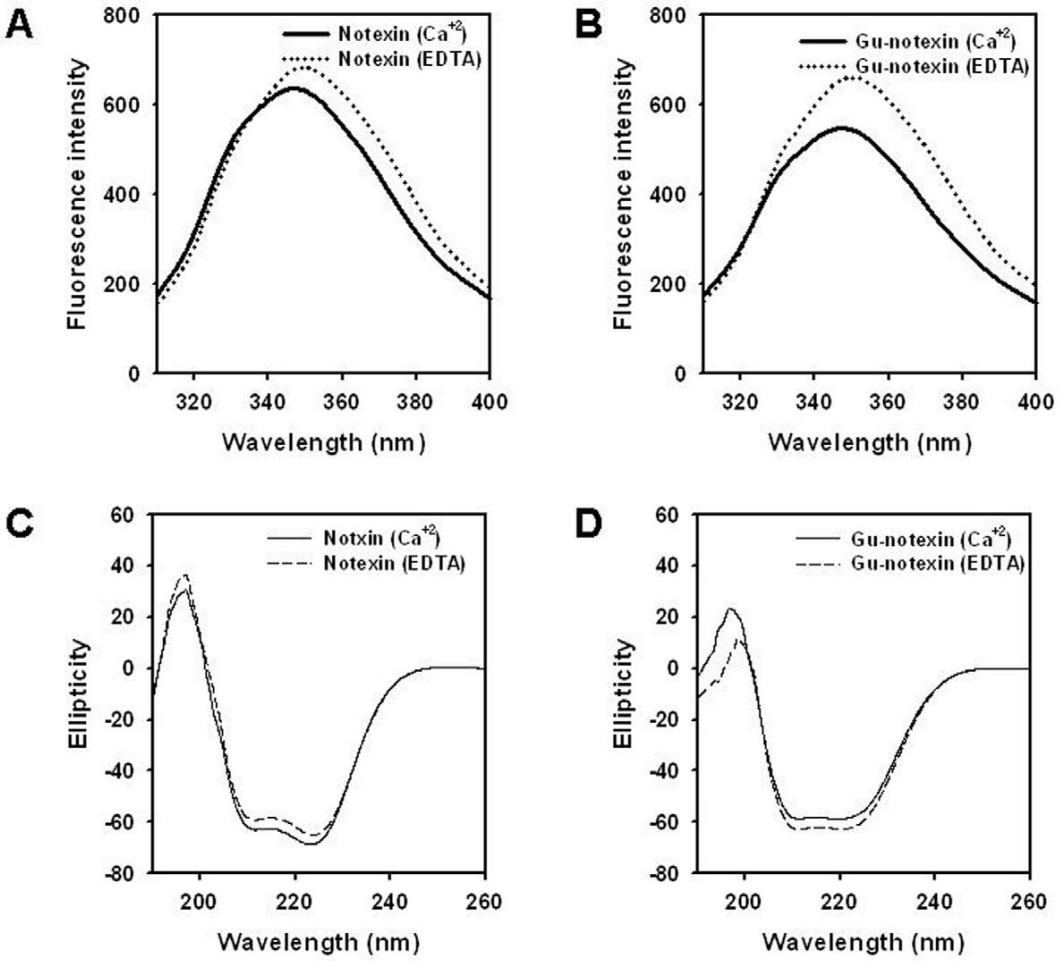

Figure 5. Trp fluorescence spectra and CD spectra of Ca^{2+}-bound notexin, metal-free notexin, Ca^{2+}-bound Gu-notexin and metal-free Gu-notexin. Notexin and Gu-notexin were dissolved in 10 mM Tris–100 mM NaCl (pH 7.5) containing 5 mM Ca^{+2} or 5 mM EDTA. Trp fluorescence spectra of notexin (**A**) and Gu-notexin (**B**) were measured using an exciting wavelength of 295 nm. Circular dichroism spectra of notexin (**C**) and Gu-notexin (**D**) were measured from 260 nm to 190 nm.

the cholesterol effect on the membrane-damaging activity of notexin and Gu-notexin, comparative studies on EYPC/EYSM (mol/mol, 70/30) and EYPC/EYSM/cholesterol (mol/mol/mol, 49/21/30) vesicles were conducted. Notexin and Gu-notexin showed a notably higher PLA_2 activity on EYPC/EYSM/cholesterol vesicles than that on EYPC or EYPC/EYSM vesicles (figure 6C). This was in line with previous studies that showed that cholesterol relieved the inhibitory effect of EYSM on PLA_2 activity (Koumanov *et al.* 1998). Nevertheless, the percentage of calcein released from EYPC/EYSM vesicles induced by Ca^{2+}-bound notexin and Gu-notexin was similar to or even greater than that from EYPC/EYSM/cholesterol vesicles (figure 6D). This indicated that PLA_2 activity did not exclusively elucidate the ability of notexin and Gu-notexin to disrupt phospholipid vesicles. Unlike that of notexin, the membrane-damaging activity of Gu-notexin toward EYPC/EYSM/cholesterol vesicles was markedly enhanced by reducing its PLA_2 activity (figure 6D). These findings suggested that guanidination promoted the ability of Ca^{2+}-free notexin to damage EYPC/EYSM/cholesterol vesicles.

Our data show that notexin and Gu-notexin could induce permeability in EYPC, EYPC/EYSM and EYPC/EYSM/cholesterol vesicles without the involvement of PLA_2 activity. Previous studies revealed that membrane-damaging activity of *Naja naja atra* and *Naja nigricollis* cardiotoxins is mediated through oligomerization and pore formation on the membrane (Chiou *et al.* 2009; Kao *et al.* 2009). Kao *et al.* (2007) proposed that notexin forms oligomeric complexes upon absorption onto the water–lipid interface. This may suggest a mode of notexin and Gu-notexin for disrupting phospholipid vesicles without the involvement of PLA_2 activity. Noticeably, guanidination of Lys residues alters global conformation and the membrane-bound mode

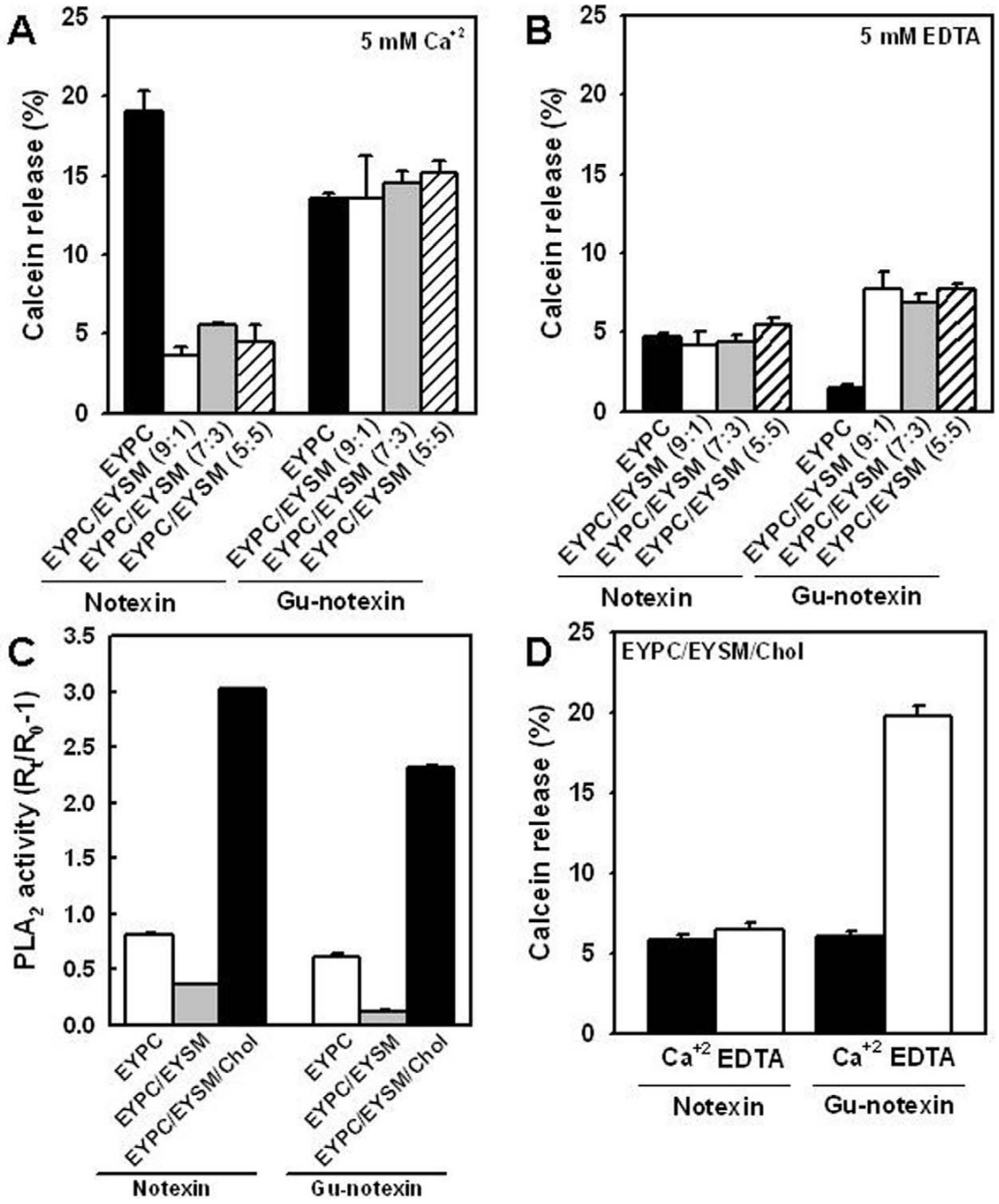

Figure 6. Effect of sphingomyelin and cholesterol on membrane-damaging activity of notexin and Gu-notexin. Notexin and Gu-notexin induced calcein release from vesicles comprising various molar ratios of EYPC and EYSM. The experiment was performed in 10 mM Tris-HCl–100 mM NaCl (pH 7.5) containing 5 mM Ca^{2+}. Notexin and Gu-notexin were added at a final concentration of 0.36 μM, and a lipid concentration of 8.14 μM. Data are presented as mean±SD of six independent experiments. (**B**) Inactivation of PLA_2 activity on membrane-damaging activity of notexin and Gu-notexin. The experiment was performed in 10 mM Tris-HCl-100 mM NaCl (pH 7.5) containing 5 mM EDTA. (**C**) Cholesterol abolished inhibitory activity of EYSM on PLA_2 activity of notexin and Gu-notexin. The concentrations of protein and lipid vesicles used were 0.36 μM and 8.14 μM, respectively. The experiment was performed in 10 mM Tris-HCl-100 mM NaCl (pH7.5) containing 5 mM Ca^{2+}. EYPC/EYSM (mol/mol, 70/30) and EYPC/EYSM/cholesterol (mol/mol/mol, 49/21/30) vesicles were used in the present experiments. The abbreviation Chol represents cholesterol. (**D**) Notexin and Gu-notexin induced calcein release from EYPC/EYSM/cholesterol (mol/mol/mol, 49/21/30) vesicles. The experiment was performed in 10 mM Tris-HCl–100 mM NaCl (pH7.5) containing 5 mM Ca^{2+} or 5 mM EDTA. The concentrations of protein and lipid vesicles were 0.36 μM and 8.14 μM, respectively.

of notexin. Compared with notexin, Gu-notexin is more effective in damaging EYPC/EYSM vesicles either in the absence or presence of Ca^{2+}. Moreover, abolition of catalytic activity results in a marked increase in Gu-notexin-induced permeability of EYPC/EYSM/cholesterol vesicles. Taken together, these suggest that, in addition to catalytic activity, membrane-bound conformation plays a vital role in the membrane-damaging activity of Gu-notexin towards EYPC/EYSM and EYPC/EYSM/cholesterol vesicles. Bakrac *et al.* (2008) suggested that specific binding of equinatoxin II with sphingomyelin is attributed to the presence of unique amido or hydroxyl groups on sphingomyelin, which is allowed to discriminate between sphingomyelin and phosphocholine below the head-group region. Alternatively, Schon *et al.* (2008) proposed that sphingomyelin functions as a specific receptor and as a promoter of membrane organization for the membrane-permeabilizing activity of equinatoxin II. The membrane-leakage action of notexin and Gu-notexin on EYPC/EYSM vesicles probably mediates partly through a similar mechanism. It is well known that packing sphingomyelin with cholesterol forms a lipid raft (Xu and London 2000). Nagahama *et al.* (2003) found that the cytotoxicity of *Clostridium perfringens* beta toxin is mediated through binding with the lipid raft, forming a functional oligomer. Moreover, the presence of membrane cholesterol in lipid raft is demonstrated to be essential for the pore formation and membrane-damaging activity of *Clostridium perfringens* beta toxin, *Clostridium perfringens* perfringolysin O, *Streptococcus intermedius* intermedilysin and *Streptococcus pyogenes* streptolysin O (Giddings *et al*. 2003; Nagahama *et al*. 2003; Heuck *et al.* 2007). Although cholesterol relieves the inhibitory effect of sphingomyelin on PLA_2 activity, notexin and Gu-notexin could induce the release of calcein from EYPC/EYSM/cholesterol vesicles underlying the deprivation of their PLA_2 activity. Thus, interaction with cholesterol or the lipid raft may be related to the membrane-permeabilizing activity of notexin and Gu-notexin. In sum, the finding that the membrane-damaging activity of notexin and Gu-notexin could proceed in a PLA_2-activity-independent manner offers an interpretation for the lack of a strict correlation between PLA_2 activity and the pharmacological activities of presynaptic PLA_2 neurotoxins. The guanidination of notexin alters its gross conformation, membrane-interaction mode and preference for damaging vesicles with different compositions. Thus, in addition to PLA_2 activity, the membrane-bound mode and phospholipid compositions of the membrane bilayers affect the membrane-damaging activity of notexin and Gu-notexin.

Acknowledgements

This work was supported by grant NSC98-2320-B110-002-MY3 from the National Science Council, ROC (to LSC), and by the grant of National Sun Yat-Sen University-Kaohsiung Medical University Joint Research Center.

References

Bakrac B, Gutierrez-Aquirre I, Podlesek Z, Sonnen A F P, Gilbert R J, Macek P, Lakey J H and Anderluh G. 2008 Molecular determinants of sphingomyelin specificity of a euksryotic pore-forming toxin; *J. Biol. Chem.* **283** 18665–18677

Chang L S 1996 Chemical modification of notexin from *Notechis scutatus scutatus* (Australian tiger snake) venom with pyridoxal-5'-phosphate; *J. Protein Chem.* **15** 473–480

Chiou Y L, Wang J J and Chang L S 2009 Effect of cholesterol on membrane-damaging activity of *Naja nigricollis* toxin γ toward phospholipid vesicles; *Toxicon* **54** 772–778

Gesquiere L, Cho W and Subbaiah P V 2002 Role of group IIa and group V secretory phospholipases A_2 in the metabolism of lipoproteins. Substrate specificities of the enzymes and the regulation of their activities by sphingomyelin; *Biochemistry* **41** 4911–4920

Giddings K S, Johnson A E and Tweten R K 2003 Redefining cholesterol's role in the mechanism of the cholesterol–dependent cytolysins; *Proc. Natl. Acad. Sci. USA* **100** 11315–11320

Gurr M I, Harwood J L and Frayn K N 2002 *Lipid Biochemistry*, fifth edition (Oxford: Blackwell Science Ltd)

Harris J B 1991 Phospholipases in snake venoms and their effect on nerve and muscle; in A L Harvey (ed.) *Snake toxins* (New York: Pergamon Press) pp 91–129

Heuck A P, Savva C G, Holzenburg A and Johnson A E 2007 Conformational changes that effect oligomerization and initiate pore formation are triggered throughout perfringolysin O upon binding to cholesterol; *J. Biol. Chem.* **282** 22629–22637

Kao P H, Lin S R and Chang L S 2007 Phospholipase A_2 activity-independent membrane-damaging effect of notexin; *Toxicon* **50** 952–959

Kao P H, Lin S R and Chang L S 2009 Differential binding to phospholipid bilayers modulates membrane-damaging activity of *Naja naja atra* cardiotoxins; *Toxicon* **54** 321–328

Kolusheva S, Shahal T and Jelinek R 2000a Peptide-membrane interactions studied by a new phospholipid/polydiacetylene colorimetric vesicles; *Biochemistry* **39** 15851–15859

Kolusheva S, Boyer L and Jelinek R 2000b A colorimetric assay for rapid screening of antimicrobial peptides; *Nat. Biotechnol.* **18** 225–227

Kolusheva S, Lecht S, Derazon Y, Jelinek R and Lazarvovici P 2008 Pardaxin, a fish toxin peptide interaction with a biomimetic phospholipid/polydiacetylene membrane assay; *Peptides* **29** 1620–1625

Koumanov K S, Quinn P J, Bereziat G and Wolf C 1998 Cholesterol relieves the inhibitory effect of sphingomyelin on type II secretory phospholipase A_2; *Biochem. J.* **336** 625–630

Ladokhin A S 1997 Distribution analysis of depth-dependent fluorescence quenching in membranes: a practical guide; *Methods Enzymol.* **278** 462–473

McIntosh T J and Holloway P W 1987 Determination of the depth of bromine atoms in bilayers formed from bromolipid probes; *Biochemistry* **26** 1783–1788

Nagahama M, Hayashi S, Morimitsu S and Sakurai J 2003 Biological activities and pore formation of *Clostridium perfringens* beta toxin in HL 60 cells; *J. Biol. Chem.* **278** 36934–36941

Paoli M, Rigoni M, Koster G, Rossetto O, Montecucco C and Postle A D 2009 Mass spectrometry analysis of phospholipase A_2 activity of snake pre-synaptic neurotoxins in cultured neurons; *J. Neurochem.* **111** 737–744.

Plant D R, Colarossi F E and Lynch G S 2006 Notexin causes greater myotoxic damage and slower functional repair in mouse skeletal muscles than bupivacaine; *Muscle Nerve* **34** 577–585.

Qin S, Pande A H, Nemec K N, He X and Tatulian S A 2005 Evidence for the regulatory role of the N-terminal helix of secretory phospholipase A_2 from studies on native and chimeric proteins; *J. Biol. Chem.* **280** 36773–36783

Ray S, Scott J L and Tatulian S A 2007 Effects of lipid phase transition and membrane surface charge on the interfacial activation of phospholipase A_2; *Biochemistry* **46** 13089–13100

Rigoni M, Schiavo G, Weston A E, Caccin P, Allegrini F, Pennuto M, Valtorta F, Montecucco C and Rossetto O 2004 Snake presynaptic neurotoxins with phospholipase A_2 activity induce punctuate swellings of neurites and exocytosis of synaptic vesicles; *J. Cell Sci.* **117** 3561–3570

Rigoni M, Caccin P, Gschmeissner S, Kdster G, Postle A D, Rossetto O, Schiavo G. and Montecucco C 2005 Equivalent effects of snake PLA_2 neurotoxins and lysophospholipid-fatty acid mixtures; *Science* **310** 1678–1680

Rosenberg P 1997 Pitfalls to avoid in the study of correlations between enzymatic activity and pharmacological properties of phospholipase A_2 enzymes; in R M Kini (ed.) *Venom phospholipase A_2 enzymes: Structure, function and mechanism* (Chichester: John Wiley) pp 155–184

Schon P, Garcia-Saez A J, Malovrh P, Bacia K, Anderluh G and Schwille P 2008 Equinatoxin II permeabilizing activity depends on the presence of sphingomyelin and lipid phase coexistence; *Biophys. J.* **95** 691–698

Surewicz W K, Mantsch H H and Chapman D 1993 Determination of protein secondary structure by Fourier transform infrared spectroscopy: a critical assessment; *Biochemistry* **32** 389–394.

Susi H, Byler D M and Purcell J M 1985 Estimation of β-structure content of proteins by means of deconvolved FTIR spectra; *J. Biochem. Biophys. Methods* **11** 235–240

Wall J, Golding C, van Veen M and O'Shea P S 1995 The use of fluoresceinphosphatidylethanolamine as a real-time probe for peptide-membrane interactions; *Mol. Membr. Biol.* **12** 181–190

Westerlund B, Nordlund P, Uhlin U, Eaker D and Eklund H 1992 The three-dimensional structure of notexin, a presynaptic neurotoxic phospholipase A_2 at 2.0 Å resolution; *FEBS Lett.* **301** 159–164

Wilson H I and Nicholson G M 1997 Presynaptic snake beta-neurotoxins produce tetanic fade and endplate potential run-down during neuromuscular blockade in mouse diaphragm; *Naunyn Schmiedebergs Arch. Pharmacol.* **356** 626–634

Xu X and London E 2000 The effect of sterol structure on membrane lipid domains reveals how cholesterol can induce lipid domain formation; *Biochemistry* **39** 843–849

Yang C C 1997 Chemical modification and functional sites of phospholipase A_2; in *Venom phospholipase A_2 enzymes: Structure, function and mechanism* (ed.) R M Kini (Chichester: John Wiley) pp 185–204

Yang C C and Chang L S 1990 The N-terminal amino group essential for the biological activity of notexin from *Notechis scutatus scutatus* venom; *Biochim. Biophys. Acta* **1040** 35–42

Zhao H and Kinnunen P K 2002 Binding of the antimicrobial peptide temporin L to liposomes assessed by Trp fluorescence; *J. Biol. Chem.* **227** 25170–25177

MS received 29 July 2010; accepted 19 October 2010

*e*Publication: 25 October 2010

Corresponding editor: Amit Chattopadhyay